

# Andrographolide suppresses thymic stromal lymphopoietin in phorbol myristate acetate/calcium ionophore A23187-activated mast cells and 2,4-dinitrofluorobenzene-induced atopic dermatitis-like mice model

Chun-xiao Li\*

Hua-guo Li\*

Hui Zhang\*

Ru-hong Cheng

Ming Li

Jian-ying Liang

Yan Gu

Bo Ling

Zhi-rong Yao

Hong Yu

Department of Dermatology, Xinhua Hospital, Shanghai Jiao Tong University School of Medicine, Shanghai, People's Republic of China

\*These authors contributed equally to this work

**Background:** Atopic dermatitis (AD) is one of the most common inflammatory cutaneous diseases. Thymic stromal lymphopoietin (TSLP) has been demonstrated to be an important immunologic factor in the pathogenesis of AD. The production of TSLP can be induced by a high level of intracellular calcium concentration and activation of the receptor-interacting protein 2/caspase-1/NF- $\kappa$ B pathway. Andrographolide (ANDRO), a natural bicyclic diterpenoid lactone, has been found to exert anti-inflammatory effects in gastrointestinal inflammatory disorders through suppressing the NF- $\kappa$ B pathway.

**Objective:** To explore the effect of ANDRO on the production of TSLP in human mast cells and AD mice model.

**Methods:** We utilized enzyme-linked immunosorbent assay, real-time reverse transcription polymerase chain reaction analysis, Western blot analysis, and immunofluorescence staining assay to investigate the effects of ANDRO on AD.

**Results:** ANDRO ameliorated the increase in the intracellular calcium, protein, and messenger RNA levels of TSLP induced by phorbol myristate acetate/calcium ionophore A23187, through the blocking of the receptor-interacting protein 2/caspase-1/NF- $\kappa$ B pathway in human mast cell line 1 cells. ANDRO, via oral or local administration, also attenuated clinical symptoms in 2,4-dinitrofluorobenzene-induced AD mice model and suppressed the levels of TSLP in lesional skin.

**Conclusion:** Taken together, ANDRO may be a potential therapeutic agent for AD through suppressing the expression of TSLP.

**Keywords:** atopic dermatitis, thymic stromal lymphopoietin, andrographolide, human mast cell

## Introduction

Atopic dermatitis (AD) is one of the most common inflammatory cutaneous diseases, characterized by chronic and relapsing eczematous skin inflammation.<sup>1</sup> The pathophysiological mechanism of AD is not fully understood; however, increasingly literature has indicated that this disease is mediated by interactions between various cells and molecular mediators.<sup>2-4</sup> Thymic stromal lymphopoietin (TSLP) was found to be an important immunologic factor in the pathogenesis of AD via enhancing the maturation of myeloid dendritic cells, which promoted the differentiation of naïve CD4<sup>+</sup> T cells into inflammatory Th2 cells.<sup>5</sup> Acute and chronic AD patients had an enhanced expression of TSLP in skin lesions.<sup>6</sup> Previous studies reported that mast cells were

Correspondence: Zhi-rong Yao; Hong Yu  
Department of Dermatology, Xinhua Hospital, Shanghai Jiao Tong University School of Medicine, 1665 Kongjiang Road, Shanghai 200092, People's Republic of China  
Fax +86 21 2507 8999  
Email zryaoxh@sina.com; smallgrass6@163.com

activated and infiltrated in the skin lesions of AD, suggesting the important role of mast cells in the pathogenesis of AD.<sup>7,8</sup> TSLP was proven to be expressed at higher levels in activated mast cells and triggered allergic inflammation.<sup>9</sup>

Caspase-1 is the best characterized inflammatory caspase.<sup>10</sup> Quite unlike the role that most caspases play in apoptosis, caspase-1 is responsible for activating the inactive precursor of interleukin (IL)-1 $\beta$ , which is vital for inflammation.<sup>11</sup> Receptor-interacting protein 2 (Rip2) is a caspase recruitment domain-containing kinase and interacts with caspase-1, thus activating the NF- $\kappa$ B signaling pathway, which has been identified to promote the transcription of *TSLP* gene in mast cells.<sup>12,13</sup>

Andrographolide (ANDRO), a natural bicyclic diterpenoid lactone, has been extracted and purified as the principal bioactive chemical ingredient from the herb *Andrographis paniculata*.<sup>14</sup> ANDRO is known to have various effects, such as antitumor,<sup>15</sup> anti-inflammatory,<sup>16</sup> and antidiabetic effects,<sup>17</sup> both in vitro and in vivo. In addition, ANDRO has been demonstrated to improve the efficacy of conventional therapy in the treatment of severe hand, foot, and mouth disease.<sup>18</sup> However, the effect of ANDRO on AD remains to be explored. Therefore, we studied the effects of ANDRO on phorbol myristate acetate/calcium ionophore A23187 (PMACI)-stimulated human mast cell line 1 (HMC-1 cells) in vitro and 2,4-dinitrofluorobenzene (DNFB)-induced AD-like lesional skin of mice in vivo.

## Materials and methods

### HMC-1 cell culture

HMC-1 cells (Cell Bank of the Chinese Academy of Science, Shanghai, People's Republic of China) were cultured in Iscove's Modified Dulbecco's Medium (Thermo Fisher Scientific, Waltham, MA, USA) containing 10% fetal calf serum (FBS, HyClone) as well as 100 U/mL penicillin and 100  $\mu$ g/mL streptomycin (Thermo Fisher Scientific). Cells were maintained in a humidified incubator at 37°C in the presence of 5% CO<sub>2</sub>.

### Fluorescent measurements of the intracellular calcium level

The intracellular calcium level was determined as described previously.<sup>19</sup> Briefly, the HMC-1 cells ( $1 \times 10^5$ ) were incubated in a culture medium containing Fura-2/AM (Sigma-Aldrich Co., St Louis, MO, USA) for 30 minutes. Then the cells were washed twice with a calcium free medium containing 0.5 mM ethylene glycol tetraacetic acid (EGTA) (Sigma-Aldrich Co.). After being placed into a 96-well plate, the cells were pretreated with ANDRO (Sigma-Aldrich Co.) of various concentrations (5, 25, 50  $\mu$ M) or 1,2-Bis(2-amino-5-methylphenoxy)ethane-N,N',N'-tetraacetic

acid tetrakis(acetoxymethyl) ester (BAPTA-AM) (10  $\mu$ M) (Sigma-Aldrich Co.) for 20 minutes and then stimulated with PMACI (50  $\mu$ M Phorbol myristate acetate + 1  $\mu$ g/mL calcium ionophore A23187) (Sigma-Aldrich Co.). The concentration of PMACI was used in subsequent experiments. The level of the intracellular calcium was measured every 10 seconds at 440 nm (excitation at 360 nm) in a spectrofluorometer. Experiments were independently repeated in triplicate.

### Cytokines assay

The levels of TSLP and IL-1 $\beta$  were determined using a sandwich enzyme-linked immunosorbent assay method according to the manufacturer's instructions (R&D Systems Inc., Minneapolis, MN, USA; Pharmingen, San Diego, CA, USA).

### RNA preparation, reverse transcription, and quantitative real-time-PCR analysis

Total RNA from tissues and cells was extracted using Trizol reagent (Thermo Fisher Scientific). RNA was reversed transcribed into cDNAs using the Primer-Script™ one step reverse transcription-polymerase chain reaction (RT-PCR) kit (TaKaRa, Dalian, People's Republic of China). The cDNA template was amplified by real-time RT-PCR using the SYBR® Premix Dimmer Eraser kit (TaKaRa). Gene expression in each sample was normalized to GAPDH expression. The primer sequences used were as follows: for GAPDH, 5'-TGGGGAAGGTGAAGGTCGG-3' (forward) and 5'-CTGGAAGATGGTGATGGGA-3' (reverse); TSLP, 5'-TATGAGTGGGACCAAAAGTACCG-3' (forward) and 5'-GGGATTGAAGGTTAGGCTCTGG-3' (reverse); and IL-1 $\beta$ , 5'-AAACAGATGAAGTGCTCCTT-3' (forward) and 5'-TGGAGAACACCACTTGTTGC-3' (reverse). The quantitative real time-PCR reaction was conducted under the following conditions: 95°C for 30 seconds, 40 cycles of 95°C for 5 seconds, and 60°C for 60 seconds. Real-time RT-PCR reactions were performed on the ABI7500 system (Thermo Fisher Scientific). The real-time PCRs were performed in triplicate. The relative expression fold change of messenger RNAs (mRNAs) was calculated by the 2<sup>- $\Delta\Delta C_t$</sup>  method.

### Cell viability assay

Cell proliferation assays were conducted using the MTT assay kits (R&D Systems Inc.) as described by the manufacturer. Briefly, HMC-1 cells were seeded into 96-well plates at a density of  $1 \times 10^4$  cells/well. HMC-1 cells were pretreated with ANDRO for 2 hours and stimulated with PMACI for 8 hours. The cells were incubated in 0.1 mg/mL MTT solution at 37°C for 4 hours and lysed in dimethyl sulfoxide at room temperature for 10 minutes. The absorbance at 540 nm in

each well was measured by a microplate reader (Bio-Rad Laboratories Inc., Hercules, CA, USA).

## Caspase-1 activity

Caspase-1 activity was performed as described previously.<sup>20</sup>

## Western blot analysis

For harvested cells, nuclear and cytosolic proteins were prepared using the NE-PER Nuclear and Cytoplasmic Fractions Kit (Thermo Fisher Scientific). Protein content was determined by Bradford assay. Equal amounts (30–50 µg) of proteins were applied to an 8%–12% SDS-polyacrylamide separating gel and transferred to a PVDF Immobilon-P membrane (Millipore, Billerica, MA, USA). The membrane was blocked with 5% skim milk in Tris-Buffered Saline and Tween 20 and then probed with the indicated primary antibodies, with gentle shaking at 4°C overnight. Primary antibodies against NF-κB (p65), IκB (1:1,000), Rip2 (1:1,000), caspase-1 (1:700), and GADPH (1:3,000) (Abcam, Cambridge, UK) were used in this study. After washing the membranes three times, the immunoblots were incubated with the appropriated goat antirabbit IgG immunoglobulins-HRP secondary antibodies (Abcam) for 1 hour. Antibody-bound proteins were detected by BeyoECL Plus kit, Haimen, People's Republic of China.

## Immunofluorescence staining

HMC-1 cells were grown on glass chamber slides for 24 hours and pretreated with ANDRO (50 µM) for 2 hours, followed by PMACI stimulation for 20 minutes. Cells were then fixed with 4% paraformaldehyde in PBS for 30 minutes. The cells were then permeabilized in 0.1% Triton X-100 (Sigma-Aldrich Co.) for 30 minutes and blocked with 0.5% bovine serum albumin (Sigma-Aldrich Co.) in PBS for 30 minutes at room temperature. After washing with PBS, the cells were incubated with anti-p65 antibody for 1 hour at room temperature. After being washed with phosphate-buffered saline with Tween 20, the cells were incubated with appropriate fluorescein isothiocyanate-conjugated secondary antibodies (Abcam) and then stained with 4',6-diamidino-2-phenylindole (Hoffman-La Roche Ltd., Basel, Switzerland). Images were later observed using a fluorescence microscope (Eclipse Ti, Nikon Corporation, Tokyo, Japan).

## Sensitization with DNFB and administration of ANDRO

BALB/c mice were obtained from animal laboratory center of Xinhua Hospital. All animal experiments were performed in the animal laboratory center of Xinhua Hospital and in accordance

with the *Guide for the Care and Use of Laboratory Animals* published by the US National Institutes of Health (NIH publication no 85–23, revised 1996). The study protocol was approved by the Animal Care and Use committee of Xinhua Hospital (approval ID: 2014012). All mice were housed in specific pathogen-free rodent facilities, on sterilized, ventilated racks and supplied with commercial chow and sterile water, both previously autoclaved. Mice were sacrificed by CO<sub>2</sub> inhalation.

The active sensitization procedure was performed as described previously.<sup>20</sup> Briefly, 100 µL 0.15% DNFB (Sigma-Aldrich Co.) dissolved in acetone was topically challenged to the shaved abdominal skins of mice on the first day. A week later, the shaved dorsal skins of mice were challenged with 100 µL 0.15% DNFB dissolved in acetone every 3 days until the 16th day. On the seventh day, ANDRO (50 mg/kg for oral, 30 mg/kg for local) or saline (control group) was administered to DNFB-challenged mice on a daily basis until the end of the experiment. In the control group, the same volume of acetone was challenged to the shaved dorsal skin and saline was administered. After anesthetization, dorsal skin samples were obtained 4 hours after the last DNFB challenge on the 16th day. The number of scratching behaviors was measured for 10 minutes, 4 hours after the last DNFB challenge.

## Histological analysis

Dorsal skin samples were embedded in paraffin, cut into 4 µm serial sections. After dewaxing and dehydration, sections were stained with hematoxylin and eosin (H&E) or toluidine blue to estimate epidermal inflammation (hypertrophy and infiltration by inflammatory cells) and mast cell counts, respectively. Epithelial thickness and the number of mast cells were determined under the inverted microscope.

## Statistical analysis

All statistical analyses were performed using SPSS 17.0 (SPSS Inc., Chicago, IL, USA). The results shown are a summary of the data from at least three experiments and are presented as mean ± standard deviation. Statistical analysis of the results was performed with an independent *t*-test. *P*-values were two-sided and a value of less than 0.05 was considered to be statistically significant.

## Results

### ANDRO decreases the intracellular calcium level and downregulates the expression of TSLP in the PMACI-activated HMC-1 cells

The chemical structure of ANDRO is shown in Figure 1A. An increase in the intracellular calcium level has been

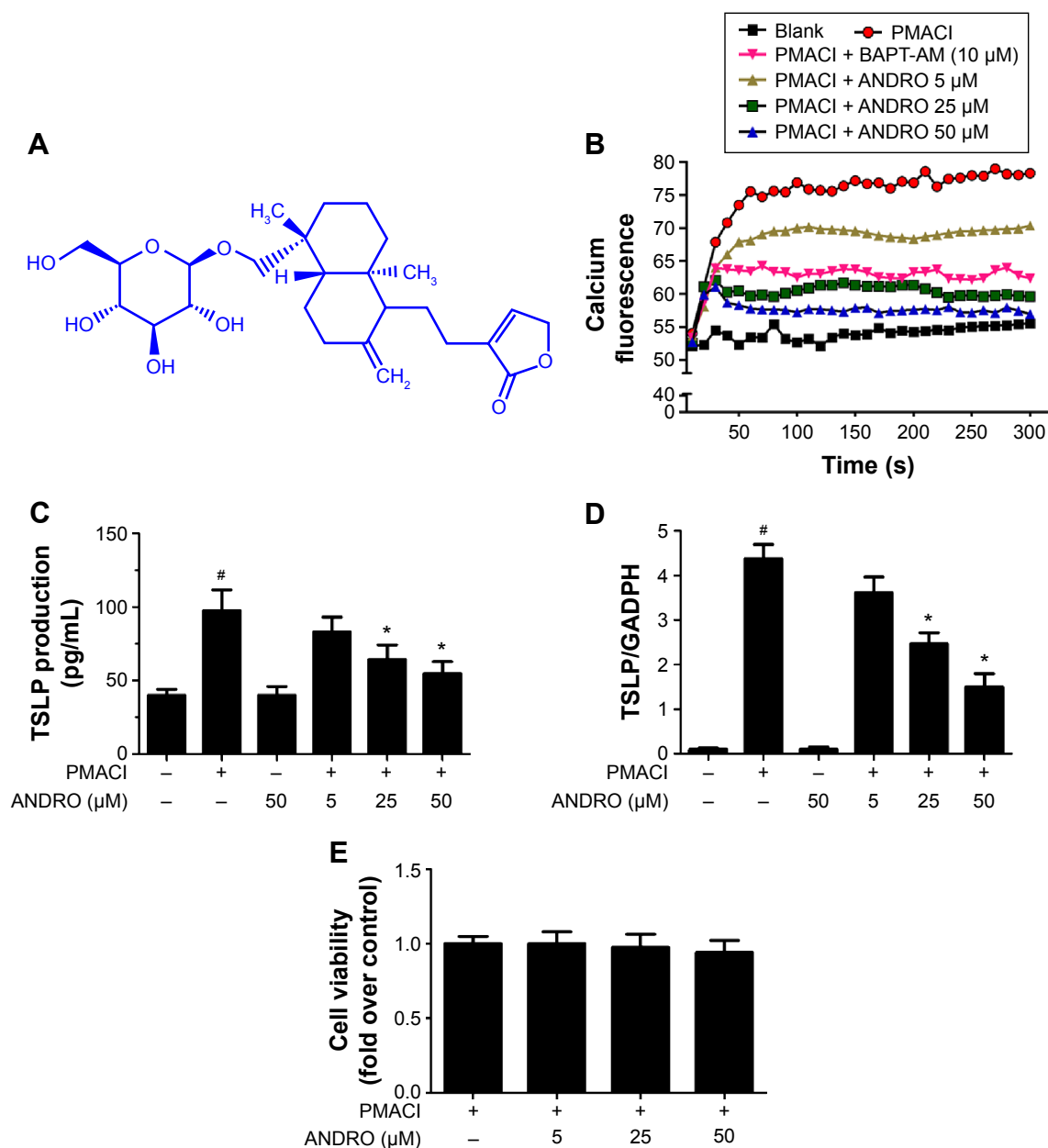


**Figure 1** Effects of ANDRO on the production and mRNA levels of TSLP in PMACI-stimulated HMC-1 cells.

**Notes:** (A) The chemical structure of ANDRO. (B) HMC-1 cells were pretreated with ANDRO (5, 25, 50  $\mu$ M) or BAPTA-AM (10  $\mu$ M) for 20 minutes and then stimulated with PMACI. The level of the intracellular calcium was measured every 10 seconds at 440 nm for 500 seconds. Blank, unstimulated cells; PMACI, PMACI-stimulated cells. (C) HMC-1 cells ( $5 \times 10^5$ ) were pretreated with ANDRO (5, 25, 50  $\mu$ M) for 2 hours and then stimulated with PMACI for 7 hours. The production of TSLP was measured with ELISA. (D) HMC-1 ( $1 \times 10^6$ ) cells were pretreated with ANDRO (5, 25, 50  $\mu$ M) for 2 hours and stimulated with PMACI for 5 hours. The transcript level of TSLP was determined with real-time PCR analysis. (E) HMC-1 cells were seeded into 96-well plates at a density of  $1 \times 10^4$  cells/well. HMC-1 cells were pretreated with ANDRO for 2 hours and stimulated with PMACI for 8 hours. Cell viability was analyzed with an MTT assay. Data represent the mean  $\pm$  standard deviation from three independent experiments.  $^{\#}P < 0.05$ , significantly different from unstimulated cells.  $^*P < 0.05$ , significantly different from PMACI-stimulated cells.

**Abbreviations:** ANDRO, andrographolide; mRNA, messenger RNA; PMACI, phorbol myristate acetate/calcium ionophore A23187; HMC-1, human mast cell line 1; PCR, polymerase chain reaction; ELISA, enzyme-linked immunosorbent assay; TSLP, thymic stromal lymphopoietin; +, chemical is added; -, chemical is absent.

shown to be a sufficient condition for the activation of mast cells and the production of a large number of cytokines.<sup>21</sup> The regulatory effect of ANDRO on the intracellular calcium level in the PMACI-activated HMC-1 cells was determined with a spectrofluorometer, and BAPTA-AM (a calcium chelator) was used as a positive control. The HMC-1 cells were pretreated with ANDRO (5, 25, 50  $\mu$ M)

or BAPTA-AM (10  $\mu$ M) for 20 minutes and then activated with PMACI. The intracellular calcium level was measured every 10 seconds at 440 nm for 500 seconds. While PMACI increased the intracellular calcium level (in 0.5 mM EGTA containing media), ANDRO attenuated its effect in a dose-dependent manner (Figure 1B). As TSLP was demonstrated to be upregulated by a high intracellular calcium level in

mast cells, we then examined the effects of ANDRO on the expression of TSLP. The HMC-1 cells were pretreated with ANDRO (5, 25, 50  $\mu\text{M}$ ) for 2 hours and then stimulated with PMACI. The ANDRO induced a significant reduction in TSLP production ( $P<0.05$ , Figure 1C) and mRNA levels ( $P<0.05$ , Figure 1D) from PMACI-activated HMC-1 cells in a dose-dependent manner. Furthermore, ANDRO exhibited no cytotoxic effects on HMC-1 cells at the above mentioned concentrations (Figure 1E).

## ANDRO inhibited the activation of the Rip2/caspase-1/NF- $\kappa\text{B}$ pathway in PMACI-activated HMC-1 cells

We would like to explore the underlying molecular mechanism through which ANDRO exerted its suppressive effects on TSLP. Previous studies have shown that the activation of the Rip2/caspase-1/NF- $\kappa\text{B}$  pathway is essential for the upregulation of TSLP.<sup>20,22,23</sup> We examined the effects that ANDRO had on the Rip2/caspase-1/NF- $\kappa\text{B}$  pathway. As illustrated in

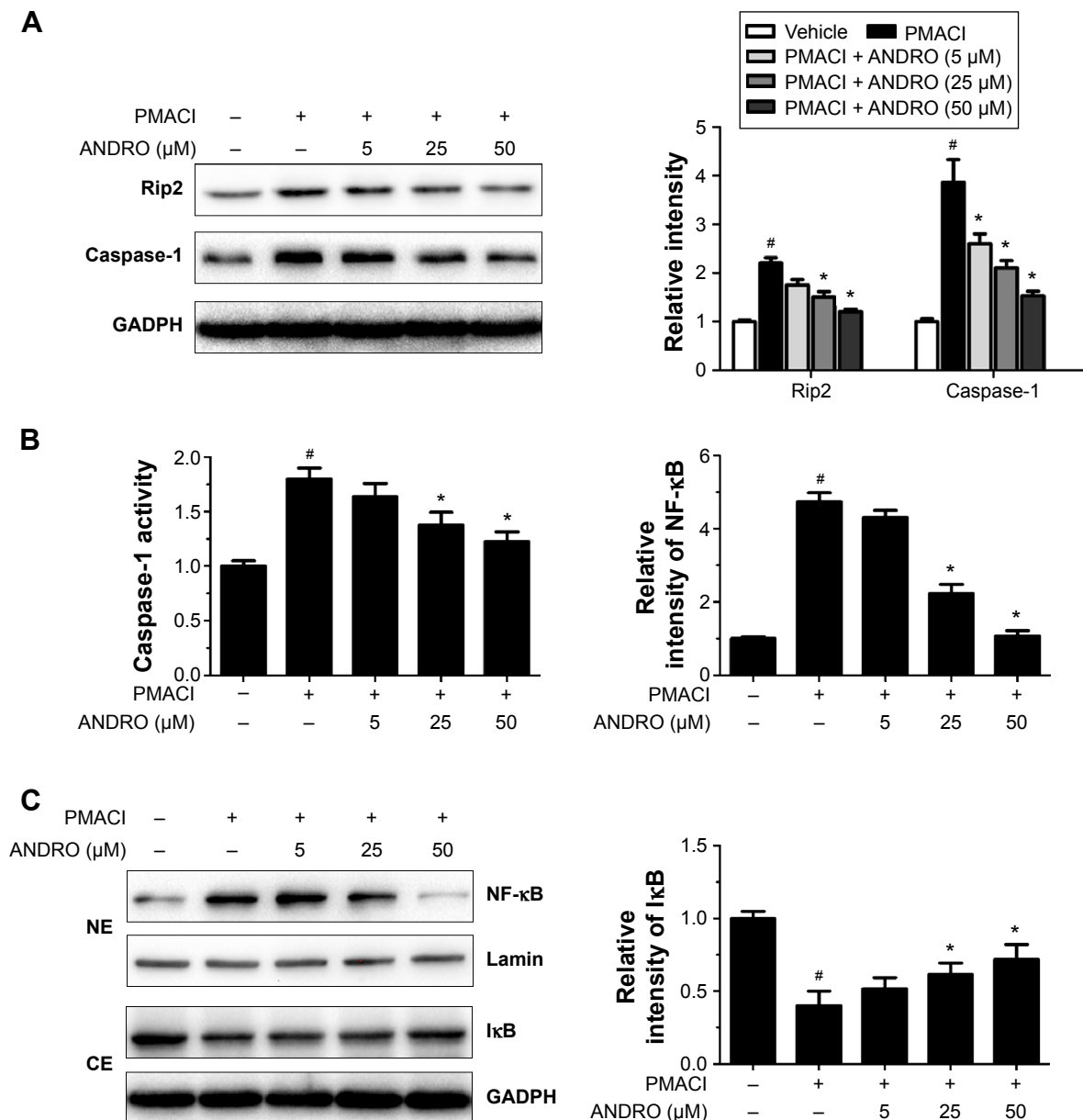


**Figure 2** ANDRO inhibited the activation of Rip2/caspase-1/NF- $\kappa\text{B}$  in PMACI-stimulated HMC-1 cells.

**Notes:** (A) HMC-1 cells were pretreated with ANDRO (5, 25, 50  $\mu\text{M}$ ) for 2 hours and stimulated with PMACI for 1 hour. Relative protein expression levels of caspase-1 and Rip2 were determined with Western blot analysis ( $n=3$ ). The relative intensities to GADPH were quantified by densitometry. (B) The caspase-1 activity was determined with a caspase-1 assay kit. (C) HMC-1 cells were pretreated with ANDRO (5, 25, 50  $\mu\text{M}$ ) for 2 hours and stimulated with PMACI for 2 hours. Relative protein expression levels of NF- $\kappa\text{B}$  and I $\kappa\text{B}$  were determined with Western blot analysis ( $n=3$ ). Data represent the mean  $\pm$  standard deviation from three independent experiments. <sup>#</sup> $P<0.05$ , significantly different from unstimulated cells. <sup>\*</sup> $P<0.05$ , significantly different from PMACI-stimulated cells.

**Abbreviations:** ANDRO, andrographolide; Rip2, Receptor-interacting protein 2; PMACI, phorbol myristate acetate/calcium ionophore A23187; HMC-1, human mast cell line 1; NE, nuclear extract; CE, cytoplasmic extract.



Figure 2A, ANDRO markedly attenuated the increase in the protein levels of Rip2 and caspase-1 induced by PMACI in a dose-dependent manner. In addition, ANDRO markedly inhibited the caspase-1 enzymatic activity (Figure 2B). In an inactivated state, NF- $\kappa$ B p65 is localized in the cytosol where it is combined with its inhibitor I $\kappa$ B. Upon phosphorylation, I $\kappa$ B is ubiquitinated and rapidly degraded, while activated

NF- $\kappa$ B p65 is translocated into the nucleus and acts as a transcriptional factor.<sup>23</sup> As shown in Figure 2C, while PMACI induced a significant increase in the content of nuclear p65 protein, ANDRO inhibited the increase in a dose-dependent manner. Such an effect of ANDRO was confirmed with the immunofluorescence analysis (Figure 3A). As illustrated in Figure 2C, PMACI-induced I $\kappa$ B degradation was markedly

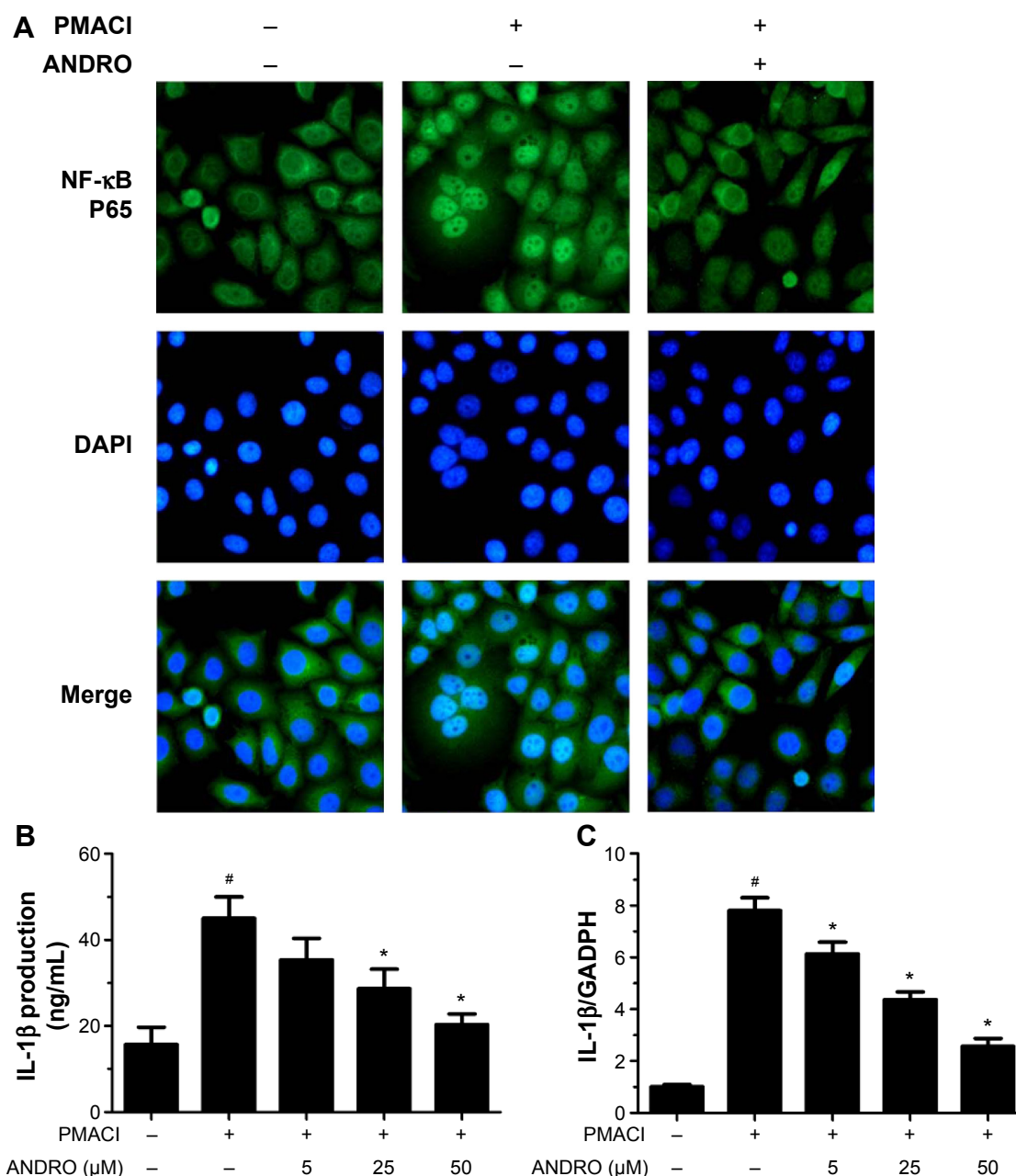


**Figure 3** ANDRO suppressed the level of nuclear NF- $\kappa$ B and IL-1 $\beta$  in PMACI-stimulated HMC-1 cells.

**Notes:** (A) HMC-1 cells pretreated with 50  $\mu$ M ANDRO for 2 hours were stimulated with PMACI for 20 minutes and processed for immunostaining with anti-p65 antibody. Nuclei of cells were stained with DAPI (blue) and p65 was visualized by green fluorescence. (B) HMC-1 cells ( $5 \times 10^5$ ) were pretreated with ANDRO (5, 25, 50  $\mu$ M) for 2 hours and then stimulated with PMACI for 7 hours. The production of IL-1 $\beta$  was measured with ELISA. (C) HMC-1 ( $1 \times 10^6$ ) cells were pretreated with ANDRO (5, 25, 50  $\mu$ M) for 2 hours and stimulated with PMACI for 5 hours. The transcript level of IL-1 $\beta$  was determined with real-time PCR analysis. Data represent the mean  $\pm$  standard deviation from three independent experiments. <sup>#</sup> $P < 0.05$ , significantly different from unstimulated cells. <sup>\*</sup> $P < 0.05$ , significantly different from PMACI-stimulated cells.

**Abbreviations:** ANDRO, andrographolide; IL, interleukin; PMACI, phorbol myristate acetate/calcium ionophore A23187; HMC-1, human mast cell line 1; PCR, polymerase chain reaction; DAPI, 4',6-diamidino-2-phenylindole; ELISA, enzyme-linked immunosorbent assay.

blocked by pretreatment with ANDRO. As caspase-1 mainly serves to cleave IL-1 $\beta$  from their inactive precursors to active forms, and NF- $\kappa$ B is a potent transcriptional factor of IL-1 $\beta$ ,<sup>24</sup> we studied whether ANDRO would have an inhibitory effect on the expression of IL-1 $\beta$ . As shown in Figure 3B and C, ANDRO markedly ameliorated the increase in the production and mRNA levels of IL-1 $\beta$  in PMACI-activated HMC-1 cells. These data suggest that ANDRO could inhibit PMACI-induced activation of the Rip2/caspase-1/NF- $\kappa$ B signaling pathway in HMC-1 cells.

### ANDRO, both orally and locally administrated, ameliorates clinical symptoms in DNFB-induced AD mice model

We then explored the regulatory effects of ANDRO on AD in vivo. Repeated skin exposure to haptens, such as DNFB, causes AD-like skin lesions in mice.<sup>20,22</sup> The TSLP expression levels in skin lesions of DNFB-induced AD-like mice were reported to be elevated.<sup>20,22</sup>

The noticeable AD-associated clinical symptoms such as erythema, excoriation, dryness, and erosion were present in DNFB-induced AD-like skin lesions; however, ANDRO, both orally and locally administrated, greatly ameliorates these symptoms in AD-like skin lesions (Figures 4A and 5A). Furthermore, ANDRO significantly relieved scratching behavior induced by DNFB (Figures 4B and 5B). We examined the thickness of the epidermis and the infiltration of inflammatory cells in skin samples from the DNFB-challenged mice, with H&E staining analysis. We also examined the infiltration of mast cells with toluidine blue staining analysis. As illustrated in Figures 4C and D and 5C and D, the epidermis thickness and the number of mast cells were greatly decreased in skin lesions from ANDRO-administrated mice, compared to that of the control group.

### ANDRO decreased the expression level of TSLP in skin lesions from DNFB-induced AD-like mice

Following this process, we examined the effects of ANDRO on TSLP expression levels in skin lesions from DNFB-induced AD-like mice. Our results revealed that ANDRO greatly suppressed the upregulation of TSLP at both mRNA and protein levels in skin lesions induced by DNFB (Figures 4E and F and 5E and F).

## Discussion

AD is one of the most common inflammatory cutaneous diseases. Although topical emollients, steroids, and oral

antihistaminic or antiallergic agents were considered to be the first-line therapy for AD patients, their long-term use could induce a variety of adverse effects.<sup>25</sup> Thus, in the search for potential new drugs for treating AD without noticeable adverse effects, traditional Chinese medicine has manifested itself with high efficacy and lower risk of adverse effects.<sup>26–28</sup> In the present study, we revealed that ANDRO has therapeutic effects on AD both in vitro and in vivo. We found that ANDRO suppressed the expression of caspase-1 and Rip2 as well as caspase-1 enzymatic activity in PMACI-activated HMC-1 cells. ANDRO also inhibited the translocation of NF- $\kappa$ B p65 into the nucleus and degradation of I $\kappa$ B induced by PMACI activation. Our study suggests that ANDRO might have a therapeutic effect on AD by downregulating TSLP via blocking the caspase-1/Rip2/NF- $\kappa$ B pathway. What is more, ANDRO, via oral and local administration, both markedly suppressed the inflammatory response induced by DNFB in vivo, as demonstrated by a decrease in the epidermis thickness and the number of inflammatory cells. ANDRO also suppressed the expression of TSLP in skin lesions induced by DNFB.

TSLP was demonstrated to play an important role in the pathogenesis of AD mainly through triggering dendritic cell-mediated Th2 inflammatory responses.<sup>5</sup> Moreover, the TSLP is produced mainly by mast cells, keratinocytes, and epithelial cells.<sup>29–31</sup> Human skin mast cells play an essential role in the pathogenesis of AD.<sup>32</sup> In this study, we focused on the TSLP produced by mast cells. An increase in the intracellular calcium level has been shown to be important for the activation of mast cells and production of a large number of cytokines, such as TSLP.<sup>21</sup> The level of TSLP was increased in stimulated HMC-1 cells.<sup>19,33</sup> Furthermore, TSLP was markedly reduced in mast cell-deficient mice.<sup>34</sup> Thus, we firstly examined whether ANDRO would attenuate the increase in the intracellular calcium level in activated HMC-1 cells. As expected, ANDRO pretreatment decreased the intracellular calcium level in PMACI-activated HMC-1 cells. In addition, ANDRO suppressed TSLP at both mRNA and protein levels in PMACI-activated HMC-1 cells.

To explore the underlying mechanism of the therapeutic effect of ANDRO on AD, we focused on the Rip2/caspase-1/NF- $\kappa$ B pathway, the activation of which has been proven to be essential for the expression of TSLP.<sup>13,22</sup> The inflammasome is a key regulator of pathogen recognition and inflammation.<sup>35</sup> Inflammasomes are multiple protein complexes that serve as molecular platforms to activate caspase-1 and regulate maturation of a potent pro-inflammatory cytokine, IL-1 $\beta$ .<sup>36</sup> Multiple key proteins of inflammasomes contain caspase recruitment domains.<sup>37</sup> Quite unlike the role that most caspases play in apoptosis, caspase-1 is responsible for activating the inactive precursor of IL-1 $\beta$ .<sup>11</sup> The NF- $\kappa$ B signaling pathway activated

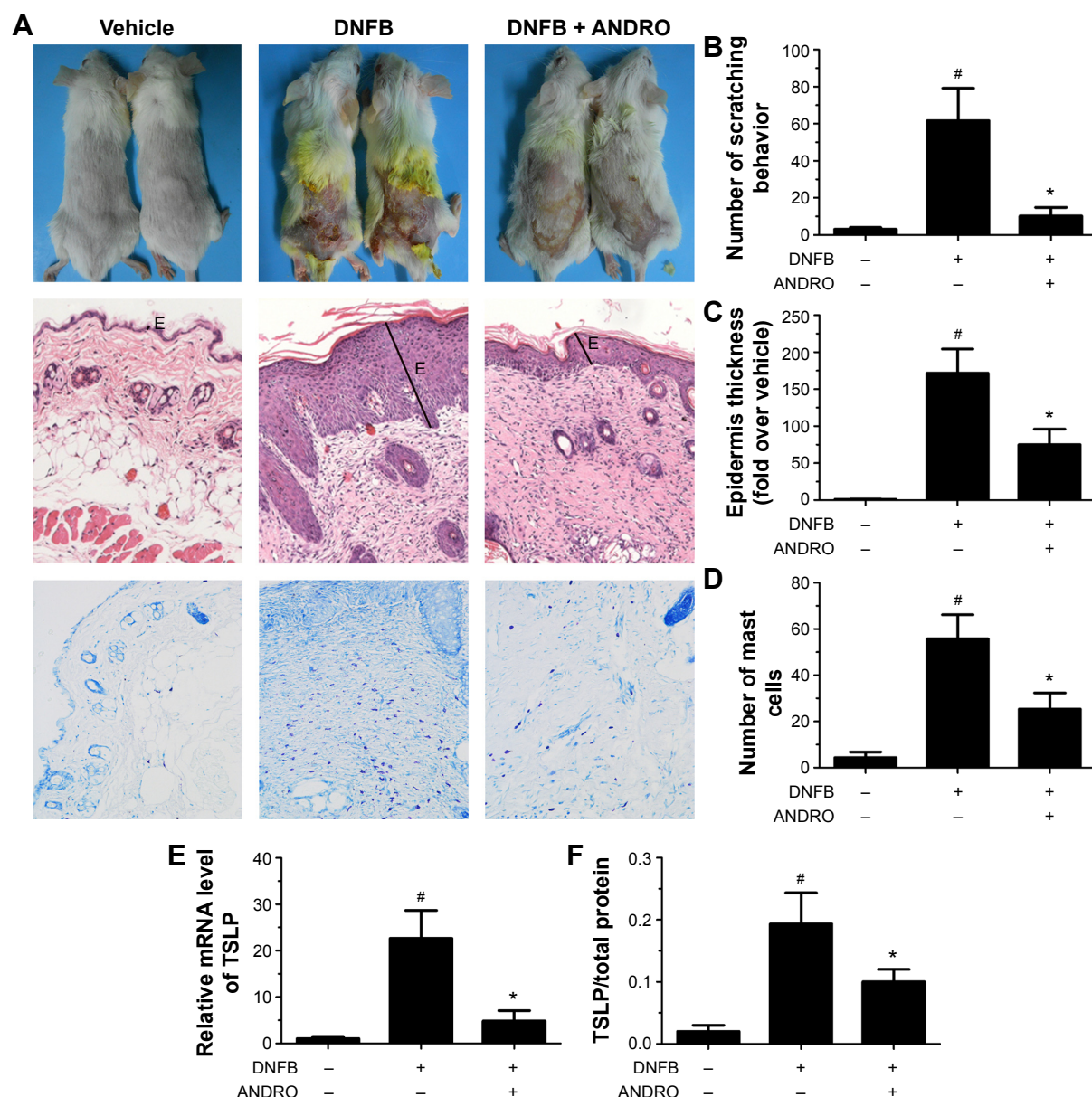


**Figure 4** ANDRO improved the clinical symptoms in DNFB-induced AD mice via oral administration.

**Notes:** ANDRO (50 mg/kg) was orally administered to DNFB-challenged mice. The clinical features were observed 4 hours after the last DNFB challenge. **(A)** Histological analysis of lesional skin was examined by H&E staining and toluidine blue staining. E indicates the epidermis. Representative photomicrographs were examined at  $\times 200$  magnification. **(B)** The number of scratching behavior of the mice was measured 4 hours after the last DNFB challenge for 10 minutes. The epidermis thickness **(C)** and the number of mast cells **(D)** were examined by H&E staining or toluidine blue staining. E indicates the epidermis. **(E)** The mRNA level of TSLP in lesional skin from DNFB-challenged AD mice was analyzed with real-time PCR. **(F)** The protein expression level of TSLP from the skin lesion homogenate was analyzed with ELISA. Data represent the mean  $\pm$  standard deviation from three independent experiments. <sup>#</sup> $P < 0.05$ , significantly different from vehicle group. <sup>\*</sup> $P < 0.05$ , significantly different from control group (DNFB-challenged),  $n = 6$ .

**Abbreviations:** ANDRO, andrographolide; DNFB, 2,4-dinitrofluorobenzene; H&E, hematoxylin and eosin; mRNA, messenger RNA; TSLP, thymic stromal lymphopoietin; AD, atopic dermatitis; PCR, polymerase chain reaction; ELISA, enzyme-linked immunosorbent assay.

by caspase-1 contributes to the production of various inflammatory cytokines, including TSLP.<sup>13</sup> Caspase-1 transgenic mice, the mice that have an enhanced expression of caspase-1, are highly susceptible to haptens and can spontaneously develop recalcitrant dermatitis and skin ulcers.<sup>38,39</sup> All these data suggest that caspase-1 is an important element in the pathogenesis of AD. Rip2 is an adaptor protein of several adaptors that compromise the inflammasome.<sup>12,40</sup> Rip2 caspase

recruitment domains interact with other caspase recruitment domain-containing proteins such as caspase-1 and lead to the activation of the NF- $\kappa$ B pathway.<sup>12,41</sup> Macrophages from Rip2-deficient mice treated with lipopolysaccharide have decreased activation of NF- $\kappa$ B.<sup>42</sup> Together, Rip2/caspase-1 pathway is important in the activation of NF- $\kappa$ B.

This study showed that ANDRO suppressed the level of TSLP by inhibiting the caspase-1/Rip2/NF- $\kappa$ B pathway.



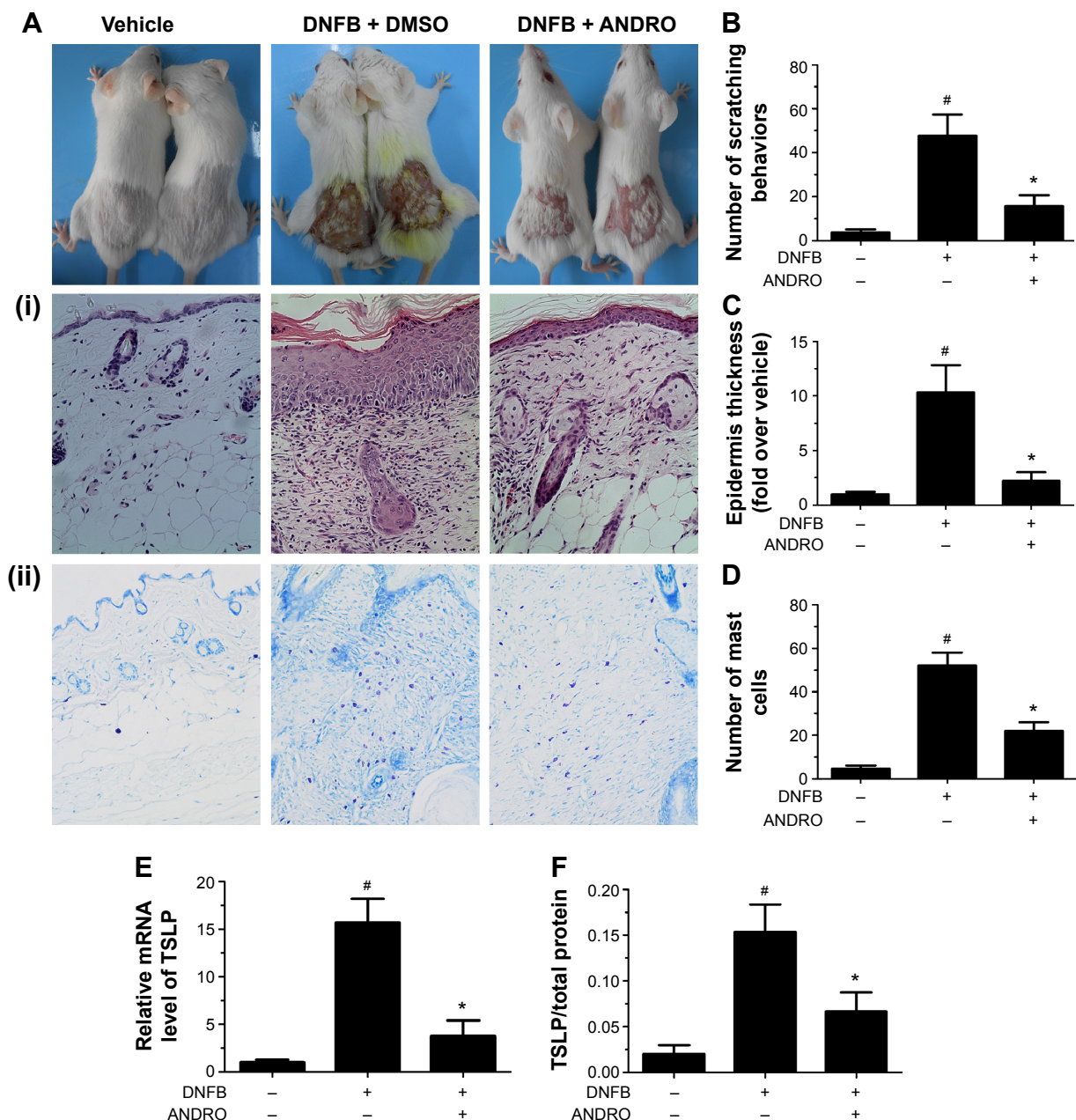


**Figure 5** ANDRO improved the clinical symptoms in DNFB-induced AD mice via local administration.

**Notes:** ANDRO (30 mg/kg) was locally administered to DNFB-challenged mice. The clinical features were observed 4 hours after the last DNFB challenge. **(A)** Histological analysis of lesional skin was examined by H&E staining (i) and toluidine blue staining (ii). Representative photomicrographs were examined at  $\times 200$  magnification. **(B)** The number of scratching behavior of the mice was measured 4 hours after the last DNFB challenge for 10 minutes. The epidermis thickness **(C)** and the number of mast cells **(D)** were examined by H&E staining or toluidine blue staining. **(E)** The mRNA level of TSLP in lesional skin from DNFB-challenged AD mice was analyzed with real-time PCR. **(F)** The protein expression level of TSLP from the skin lesion homogenate was analyzed with ELISA. Data represent the mean  $\pm$  standard deviation from three independent experiments. <sup>#</sup> $P < 0.05$ , significantly different from vehicle group. <sup>\*</sup> $P < 0.05$ , significantly different from control group (DNFB-challenged),  $n = 6$ .

**Abbreviations:** ANDRO, andrographolide; DMSO, Dimethyl sulfoxide; DNFB, 2,4-dinitrofluorobenzene; H&E, hematoxylin and eosin; mRNA, messenger RNA; TSLP, thymic stromal lymphopoietin; AD, atopic dermatitis; PCR, polymerase chain reaction; ELISA, enzyme-linked immunosorbent assay.

These results suggest that ANDRO might be a potential therapeutic agent for AD.

## Acknowledgments

This work was supported by National Natural Science Foundation of China for the Youth (81201227), Science

and Technology Commission of Shanghai Municipality (12411951600, 13XD1402900), and 2016 CMA-L'OREAL China Skin Grant (S2016131417). The funding sources had no role in the study design; collection, analysis, and interpretation of data; writing of the manuscript; and decision to submit the manuscript for publication.

## Disclosure

The authors report no conflicts of interest in this work.

## References

- Schmitt J, Langan S, Deckert S, et al; Harmonising Outcome Measures for Atopic Dermatitis (HOME) Initiative. Assessment of clinical signs of atopic dermatitis: a systematic review and recommendation. *J Allergy Clin Immunol*. 2013;132:1337–1347.
- Harskamp CT, Armstrong AW. Immunology of atopic dermatitis: novel insights into mechanisms and immunomodulatory therapies. *Semin Cutan Med Surg*. 2013;32:132–139.
- Kawakami T, Ando T, Kimura M, Wilson BS, Kawakami Y. Mast cells in atopic dermatitis. *Curr Opin Immunol*. 2009;21:666–678.
- Yamanaka K, Mizutani H. The role of cytokines/chemokines in the pathogenesis of atopic dermatitis. *Curr Probl Dermatol*. 2011;41:80–92.
- Jariwala SP, Abrams E, Benson A, Fodeman J, Zheng T. The role of thymic stromal lymphopoietin in the immunopathogenesis of atopic dermatitis. *Clin Exp Allergy*. 2011;41:1515–1520.
- Lee J, Noh G, Lee S, Youn Y, Rhim J. Atopic dermatitis and cytokines: recent patents in immunoregulatory and therapeutic implications of cytokines in atopic dermatitis – part I: cytokines in atopic dermatitis. *Recent Pat Inflamm Allergy Drug Discov*. 2012;6:222–247.
- Harvima IT, Nilsson G. Mast cells as regulators of skin inflammation and immunity. *Acta Derm Venereol*. 2011;91:644–650.
- Liu FT, Goodarzi H, Chen HY. IgE, mast cells, and eosinophils in atopic dermatitis. *Clin Rev Allergy Immunol*. 2011;41:298–310.
- Indra AK. Epidermal TSLP: a trigger factor for pathogenesis of atopic dermatitis. *Expert Rev Proteomics*. 2013;10:309–311.
- Lamkanfi M, Vande Walle L, Kanneganti TD. Deregulated inflammasome signaling in disease. *Immunol Rev*. 2011;243:163–173.
- Boost KA, Hoegl S, Hofstetter C, et al. Targeting caspase-1 by inhalation-therapy: effects of Ac-YVAD-CHO on IL-1 beta, IL-18 and downstream proinflammatory parameters as detected in rat endotoxaemia. *Intensive Care Med*. 2007;33:863–871.
- Staal J, Bekaert T, Beyaert R. Regulation of NF- $\kappa$ B signaling by caspases and MAL1 paracaspase. *Cell Res*. 2011;21:40–54.
- Moon PD, Kim HM. Thymic stromal lymphopoietin is expressed and produced by caspase-1/NF- $\kappa$ B pathway in mast cells. *Cytokine*. 2011;54:239–243.
- Bao GQ, Shen BY, Pan CP, et al. Andrographolide causes apoptosis via inactivation of STAT3 and Akt and potentiates antitumor activity of gemcitabine in pancreatic cancer. *Toxicol Lett*. 2013;222:23–35.
- Zhang QQ, Ding Y, Lei Y, et al. Andrographolide suppress tumor growth by inhibiting TLR4/NF- $\kappa$ B signaling activation in insulinoma. *Int J Biol Sci*. 2014;10:404–414.
- Liu W, Guo W, Guo L, et al. Andrographolide sulfonate ameliorates experimental colitis in mice by inhibiting Th1/Th17 response. *Int Immunopharmacol*. 2014;20:337–345.
- Nugroho AE, Lindawati NY, Herlyanti K, Widyastuti L, Pramono S. Anti-diabetic effect of a combination of andrographolide-enriched extract of *Andrographis paniculata* (Burm f.) Nees and asiaticoside-enriched extract of *Centella asiatica* L. in high fructose-fat fed rats. *Indian J Exp Biol*. 2013;51:1101–1108.
- Li X, Zhang C, Shi Q, et al. Improving the efficacy of conventional therapy by adding andrographolide sulfonate in the treatment of severe hand, foot, and mouth disease: a randomized controlled trial. *Evid Based Complement Alternat Med*. 2013;2013:316250.
- Han NR, Kim HM, Jeong HJ. Thymic stromal lymphopoietin is regulated by the intracellular calcium. *Cytokine*. 2012;59:215–217.
- Han NR, Moon PD, Kim HM, Jeong HJ. Tryptanthrin ameliorates atopic dermatitis through down-regulation of TSLP. *Arch Biochem Biophys*. 2014;542:14–20.
- Ma HT, Beaven MA. Regulators of Ca(2+) signaling in mast cells: potential targets for treatment of mast cell-related diseases? *Adv Exp Med Biol*. 2011;716:62–90.
- Han NR, Kang SW, Moon PD, Jang JB, Kim HM, Jeong HJ. Genuine traditional Korean medicine, Naju Jjok (Chung-Dae, Polygonum tinctorium) improves 2,4-dinitrofluorobenzene-induced atopic dermatitis-like lesional skin. *Phytomedicine*. 2014;21:453–460.
- Heymann MC, Winkler S, Luksch H, et al. Human procaspase-1 variants with decreased enzymatic activity are associated with febrile episodes and may contribute to inflammation via RIP2 and NF- $\kappa$ B signaling. *J Immunol*. 2014;192:4379–4385.
- Zhu C, Xiong Z, Chen X, et al. Artemisinin attenuates lipopolysaccharide-stimulated proinflammatory responses by inhibiting NF- $\kappa$ B pathway in microglia cells. *PLoS One*. 2012;7(4):e35125.
- Berke R, Singh A, Guralnick M. Atopic dermatitis: an overview. *Am Fam Physician*. 2012;86:35–42.
- Wu CT, Huang KS, Yang CH, et al. Inhibitory effects of cultured *Dendrobium tosaense* on atopic dermatitis murine model. *Int J Pharm*. 2014;463:193–200.
- Li S, Kuchta K, Tamaru N, et al. Efficacy of a novel herbal multi-component traditional Chinese medicine therapy approach in patients with atopic dermatitis. *Forsch Komplementmed*. 2013;20:189–196.
- Gu S, Yang AW, Xue CC, et al. Chinese herbal medicine for atopic eczema. *Cochrane Database Syst Rev*. 2013;9:CD008642.
- Yamamoto-Kasai E, Yasui K, Shichijo M, Sakata T, Yoshioka T. Impact of TRPV3 on the development of allergic dermatitis as a dendritic cell modulator. *Exp Dermatol*. 2013;22(12):820–824.
- Jia X, Zhang H, Cao X, Yin Y, Zhang B. Activation of TRPV1 mediates thymic stromal lymphopoietin release via the Ca2+/NFAT pathway in airway epithelial cells. *FEBS Lett*. 2014;588(17):3047–3054.
- Wilson SR, Thé L, Batia LM, et al. The epithelial cell-derived atopic dermatitis cytokine TSLP activates neurons to induce itch. *Cell*. 2013;155(2):285–295.
- Kritas SK, Saggini A, Varvara G, et al. Impact of mast cells on the skin. *Int J Immunopathol Pharmacol*. 2013;26:855–859.
- Han NR, Kim HM, Jeong HJ. The  $\beta$ -sitosterol attenuates atopic dermatitis-like skin lesions through down-regulation of TSLP. *Exp Biol Med (Maywood)*. 2014;239:454–464.
- Takai T. TSLP expression: cellular sources, triggers, and regulatory mechanisms. *Allergol Int*. 2012;61:3–17.
- Dai X, Sayama K, Tohyama M, et al. Mite allergen is a danger signal for the skin via activation of inflammasome in keratinocytes. *J Allergy Clin Immunol*. 2011;127:806–814.
- Leavy O. Inflammasomes: polymeric assembly. *Nat Rev Immunol*. 2014;14:287.
- Mariathasan S, Newton K, Monack DM, et al. Differential activation of the inflammasome by caspase-1 adaptors ASC and Ipaf. *Nature*. 2004;430:213–218.
- Yamanaka K, Tanaka M, Tsutsui H, et al. Skin-specific caspase-1-transgenic mice show cutaneous apoptosis and pre-endotoxin shock condition with a high serum level of IL-18. *J Immunol*. 2000;165:997–1003.
- Murakami T, Yamanaka K, Tokime K, et al. Topical suplatast tosilate (IPD) ameliorates Th2 cytokine-mediated dermatitis in caspase-1 transgenic mice by downregulating interleukin-4 and interleukin-5. *Br J Dermatol*. 2006;155:27–32.
- Thome M, Hofmann K, Burns K, et al. Identification of CARDIAK, a RIP-like kinase that associates with caspase-1. *Curr Biol*. 1998;8:885–888.
- McCarthy JV, Ni J, Dixit VM. RIP2 is a novel NF- $\kappa$ B-activating and cell death-inducing kinase. *J Biol Chem*. 1998;273:16968–16975.
- Chin AI, Dempsey PW, Bruhn K, Miller JF, Xu Y, Cheng G. Involvement of receptor-interacting protein 2 in innate and adaptive immune responses. *Nature*. 2002;416:190–194.

**Drug Design, Development and Therapy****Dovepress****Publish your work in this journal**

Drug Design, Development and Therapy is an international, peer-reviewed open-access journal that spans the spectrum of drug design and development through to clinical applications. Clinical outcomes, patient safety, and programs for the development and effective, safe, and sustained use of medicines are a feature of the journal, which

has also been accepted for indexing on PubMed Central. The manuscript management system is completely online and includes a very quick and fair peer-review system, which is all easy to use. Visit <http://www.dovepress.com/testimonials.php> to read real quotes from published authors.

Submit your manuscript here: <http://www.dovepress.com/drug-design-development-and-therapy-journal>